CHEMIN: A Miniaturized X-ray Diffraction and X-ray Fluorescence Instrument

D. L. Bish (bish@lanl.gov), S. J. Chipera, and D. T. Vaniman (EES-6)

Approximately 100 elements exist in our universe, and these elements can combine to form at least 3,800 minerals (naturally formed crystals). Using chemical analysis, one can identify the elements in a material, but most often, this method cannot be used to identify the crystalline structure, which can be crucial for establishing the properties of a mineral or synthetic crystal. In addition, knowing which minerals are present in a sample can help determine the mineral's alteration history. In this article, we will discuss CHEMIN, a prototype miniature instrument we developed that can identify both the CHEMistry and MINeralogy (crystalline structure) of a sample.

CHEMIN was originally developed for space travel to Mars and is the first miniature instrument to perform these two identifications using both x-ray diffraction (XRD) and x-ray fluorescence (XRF) analysis. In 1999, we received an R&D 100 award for the CHEMIN instrument. Its potential uses extend far beyond Mars to many applications on Earth, including portable field instruments, robots that analyze contaminants in hazardous areas, and machines that perform on-line analyses of solid phases in production facilities.

History

Geoscientists in EES Division have been interested in miniaturized XRD/XRF instrumentation since 1990. Early in the decade, research in our division focused on both isotopic and tube-source instruments, as well as a variety of detector systems integrated in an instrument that passed x-rays through a sample (transmission geometry) rather than diffracting them off the sample (reflection geometry). At this time, we are improving CHEMIN as a potential flight instrument for the exploration of extraterrestrial bodies.

Space Exploration

The origins and histories of planetary, asteroidal, and cometary bodies are reflected in their constituent minerals. This tremendous variety of mineralogy carries stories of pressure, temperature, oxygen fugacity, and solution chemistry, all intertwined with histories of sedimentation, igneous activity, metamorphism, impacts, and surface weathering. The science objectives of determining simultaneous chemistry and mineralogy thus span the full history of planetary, asteroidal, and cometary formation and evolution. Fegley et al. suggested in 1992 that the CHEMIN concept could be a valuable means to resolve mineralogic uncertainties for Venus. More recently, it was pointed out by Rietmeijer that to perform successful in situ study of an active comet nucleus, one must use an instrument like CHEMIN for unambiguous mineral identification.

The CHEMIN Instrument

CHEMIN is a miniaturized, simultaneous-XRD/XRF instrument based on a charge-coupled device

Figure 1. CHEMIN Instrument.
The prototype with collimator and sample holder on the left and charge-coupled device (CCD) on the right.

(CCD) that exists in prototype form (Figure 1). The intrument is designed to characterize elemental composition and mineralogy from small fine-grained or powder samples.

We have obtained usable diffraction data from the instrument in only a few minutes, and we predict that a flight instrument should be able to collect data in 1 to 2 hours. CHEMIN discriminates between diffracted and fluoresced x-rays by operating the CCD in what is known as “single-photon-counting” mode, with photons of the x-ray tube characteristic energy (e.g., Cu Kα or Cu Kβ) ascribed to diffraction events. The instrument is operated in this mode by exposing the CCD detector to repeated short bursts of x-rays. When using short exposure times (~10 to 60 s), ideally no more than one photon strikes each pixel (or picture element) of the 512×512 pixel CCD. Under these conditions, the charge deposited in each pixel is proportional to the energy of the x-ray photon striking the pixel, providing the option to analyze the photon energy on a pixel-by-pixel basis.

CHEMIN distinguishes between diffracted characteristic photons and fluorescence photons based on the fact that diffracted photons have the characteristic energy of the incident x-rays whereas fluorescence x-rays are characteristic of the sample chemistry and have different energies (Figure 2).

The XRD data, which are measured in transmission geometry, yield concentric rings on the CCD detector (Figure 2), providing information on phase structure. The XRF signals strike the CCD uniformly across the detector and can be combined to provide elemental information. The CCD detector in our current design is encased in an instrument measuring $15 \times 12 \times 22$ cm. A flight instrument would weigh less than 1 kg, have a volume of 500 cm^3, and have power requirements of 2 W.

Figure 3 shows the spatial relationships between components in existing CHEMIN instruments. The advanced CHEMIN instrument, capable of operating in space or remotely on earth is illustrated in Figure 4. It is can be described as a series of subsystems: (1) an x-ray tube source, (2) a sample-manipulation system, and (3) a CCD detector that simultaneously records both energy and position of x-rays on the two-dimensional CCD detector.

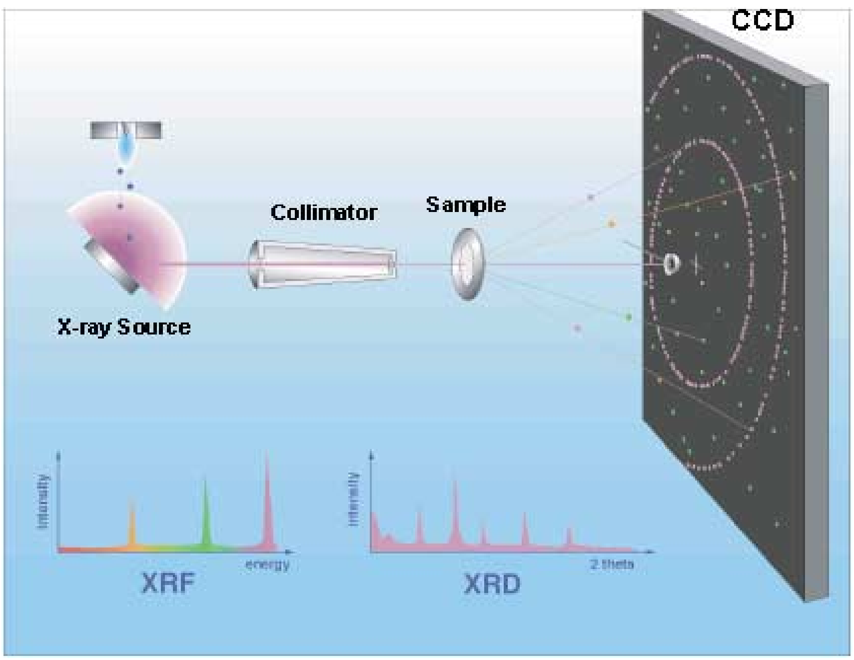

Figure 2. Generation and Measurement of X-ray Diffraction and Fluorescence Signals from a Single Sample.
X-rays impinging on the CCD detector are indicated by colored dots, and their energy distribution is shown at the bottom in the XRF spectrum. The violet dots indicate the diffracted x-rays that are characteristic of the x-ray source and, hence, diffracted from the sample. Dots of other colors do not fall in a fixed pattern and represent x-rays fluoresced from various elements within the sample. Note that the violet dots fall in a pattern of concentric circles, the position of which is reflective of the crystal structure of the sample. The two-dimensional XRD pattern at the bottom, obtained by circumferential integration of the violet rings, corresponds to a conventional XRD pattern.

Field-Emission X-ray Tube. At present, a standard laboratory x-ray tube is used with CHEMIN. The x-ray source component is shown as a standard tube in Figure 3. For a flight instrument, we propose using a sealed, high-vacuum envelope housing a micromachined-field-emitter (MMFE) array, an electrostatic focusing element, and an anode, onto which a small focused beam of electrons is accelerated. The MMFE concept has already been used successfully in devices such as flat-panel color monitors. In operating mode, a continuous electrostatic potential of 20 keV is applied between the anode and the MMFE array, and an electron current is created by impressing a potential of ~50 V on the extraction anode of the MMFE array.

Sample-Manipulation System. Mechanical handling of rock, soil, and ice samples is one of the more difficult problems in robotic analysis of extraterrestrial bodies. Both eolian dusts and soils can be collected easily and analyzed without extensive processing; however, to analyze solid geologic media fully, one will almost always require a method to obtain the geologic media in powder form. We are considering two methods for obtaining powders: piezoelectric microdrilling and explosive powdering systems. Both methods have been developed and have prototype systems available that can be tested against a variety of target lithologies.

CCD Detector Array. The third component and the heart of CHEMIN is the CCD detector array and electronics. The ideal CCD would be based on the CUBIC (cosmic undefined background instrument with CCDs) detector built and flown by the Jet Propulsion Laboratory in their x-ray astronomy studies. The array in the planned instrument consists of a matrix of 1024 × 1024 pixels in a front-illuminated CCD. Important characteristics of the device are listed in Tables 1 and 2. In most applications, CHEMIN can be operated in shaded or in local nighttime Martian conditions, when the ambient temperature is sufficiently low to reduce background to an acceptable level without any additional cooling.

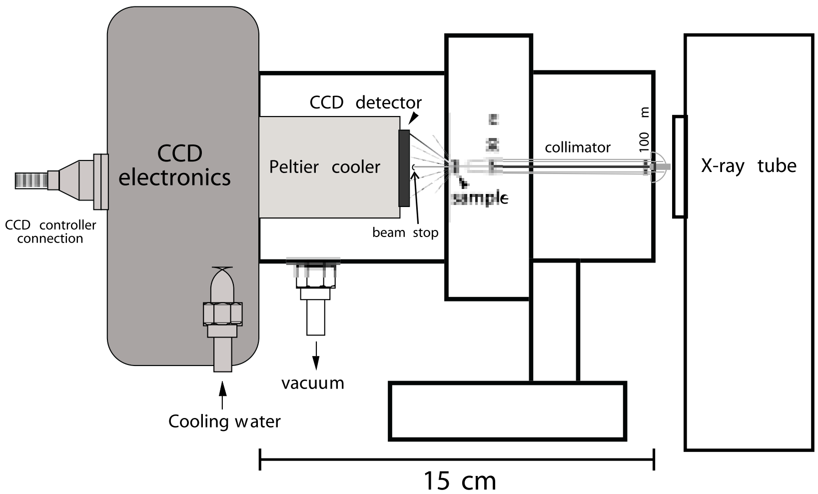

Figure 3. Prototype CHEMIN. Schematic of the existing instrument.

Data Collection and Analysis

During data collection, a collimated x-ray beam strikes a thin-film substrate sample holder held in the second component of the system, which is a multiposition sample carousel. The carousel disc is the only moving part in the CHEMIN instrument. The carousel can be precisely and continuously rotated 360° by a stepper motor. The substrates are x-ray-thin (~2 µm) Mylar films made sticky on the top surface by a thin film of vacuum grease or the like. A protective cover is removed from the greased Mylar as it advances into the sample collection port. A sample is dumped into the sample collection port, and powder adheres to the sticky surface of the Mylar, whereas excess powder and larger grains roll off the inclined substrate. The carousel is then rotated into position for analysis between the x-ray source and the CCD detector array. While in the position for analysis, 50-µm diameter regions are illuminated by the collimated x-ray beam. Approximately 50 exposures are collected of each area, after which the motor steps ~100 µm so that a new area of sample material on the same substrate is analyzed. An “exposure” is made by providing a pulse of 50 V to the extraction anode of the x-ray tube, flooding the CCD with diffracted and fluoresced x-ray photons. As we already mentioned, the CCD is operated in single-photon counting mode to measure both diffraction and fluorescence data simultaneously.

Figure 5 illustrates the flat-plate diffraction data obtained for Al_2O_3 from CHEMIN, before circumferential integration. CHEMIN’s diffraction methodology is particularly good with poorly prepared samples such as natural dusts or soils. The advantage of the CHEMIN geometry is illustrated in Figure 6, which

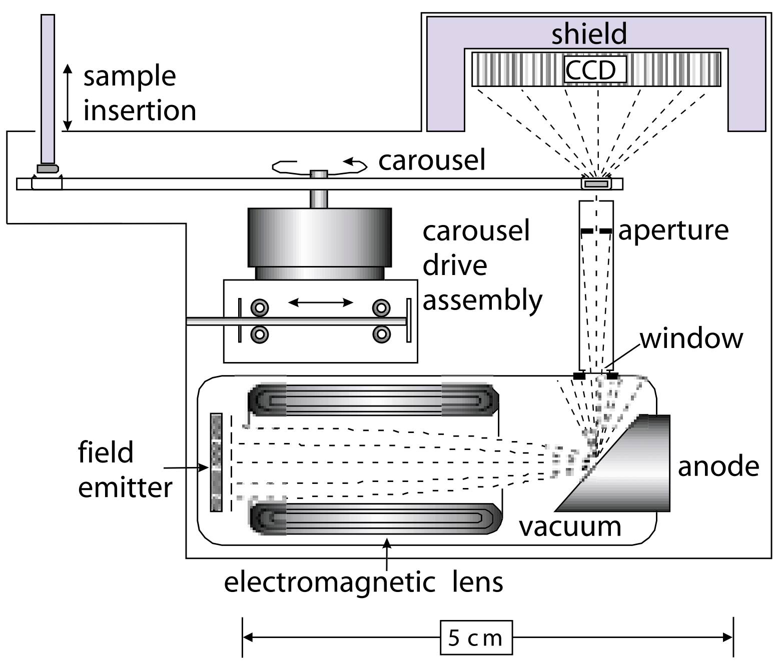

Figure 4. Advanced CHEMIN.
Schematic of the proposed advanced CHEMIN instrument showing the spatial relationships among the three components that are critical to the operation of CHEMIN.

Table 1. Characteristics of the Proposed CHEMIN CCD

Format	1024 x 1024
Pixel size (µm)	18
Number of readout channels	4
Readout noise, e⁻ (rms)	0.5

Energy (eV)	Quantum Efficiency	Energy Resolution (FWHM) (eV)
277	0.15	38
1000	0.70	60
5400	0.15	115
8000	0.05	130

Table 2. Overall Instrument Parameters for Proposed CHEMIN

Detector	X-ray sensitive (thin polygate) CCD
X-ray tube electron source	Field-effect emitter array
Range (degrees 2θ)	5 to 55°
Diffraction resolution	<0.2° 2θ
Mass (kg)	0.8
Power (W)	2.0

shows a CHEMIN XRD pattern of aragonite at the top. CHEMIN accumulates part or all of the Debye rings out to about 50° 2θ (Cu Kα). Circumferential integration of each ring compensates for poor powder preparation (i.e., spotty Debye rings), such as might be produced by robotic sampling systems. Simulations of conventional diffractometer data (stippled line) and Debye-Scherrer film data are shown at the bottom of Figure 6, illustrating the loss of diffraction signal averaging that can take place when the full Debye rings are not used.

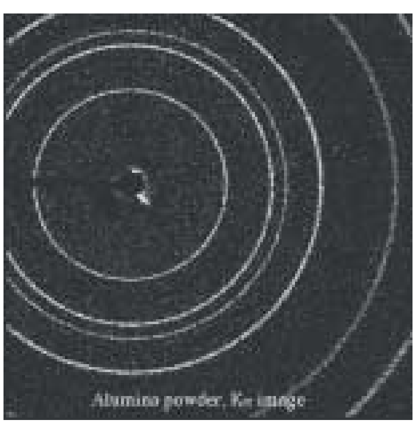

Figure 5. Flat-plate Diffraction.
Data for Al_2O_3 (corundum) obtained using the prototype CHEMIN instrument.

Further data processing using circumferential integration produces a diffraction pattern like that shown in Figure 7, which illustrates a comparison between the CHEMIN diffraction pattern of quartz and the pattern obtained on a conventional laboratory diffractometer. XRF data as well as XRD data are collected even with the test CCD in CHEMIN at the Los Alamos National Laboratory, although XRF data of higher quality are obtained with the CUBIC CCD at the Jet Propulsion Laboratory. An example of an XRF spectrum measured on aragonite, $CaCO_3$, is shown in Figure 8. The spectrum is remarkable in the presence of the C and O lines, in addition to Ca; Cu and Al arise from the sample holder. Conventional x-ray fluorescence instruments are typically incapable of detecting C and O x-rays.

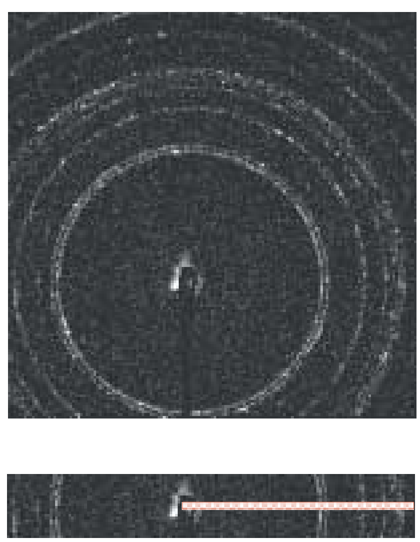

Figure 6. Comparison of Techniques.
The figure shows relative amounts of diffraction data for aragonite resulting from CHEMIN (upper square), a Debye-Scherrer camera (lower strip), and a conventional laboratory diffractometer (stippled red region).

Advantages of CHEMIN

In Table 3, we compare two XRD analyses with a normative calculation for a terrestrial basalt sample. We obtained one of the XRD analyses with the prototype CHEMIN instrument (Figures 1 and 3); the other we obtained with a Siemens laboratory diffractometer. Although the CHEMIN analysis has poorer peak resolution, the data we obtained are sufficient not only to determine the mineral phases present but also to apply Rietveld analysis to estimate the relative proportions of mineral phases in the sample. (Rietveld analysis involves calculating a model diffraction pattern based on the crystal structures of the known phases in a mixture. The quality of fit between the observed and calculated diffraction patterns is then improved using a least-squares process in which relative amounts of each phase and the crystal structural parameters are varied.)

We have developed software to combine both the chemical XRF data and the XRD data to perform this operation more rigorously. The analysis represented in Figure 9 uses only the XRD data. The goodness of fit for a Rietveld analysis of the XRD data is usually expressed using statistical parameters but can also be visualized as a difference pattern, shown at the bottom of Figure 9.

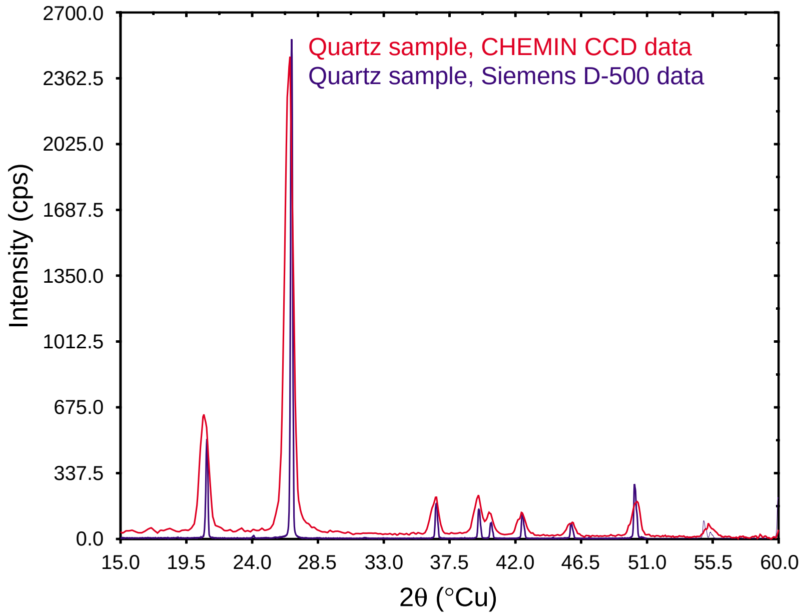

Figure 7. Quartz Diffraction.
Diffraction pattern of quartz from circumferential integration of flat-plate CHEMIN data (red) compared with pattern from a conventional laboratory diffractometer (blue).

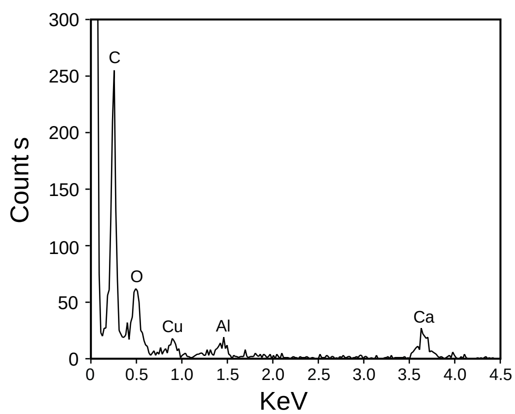

Figure 8. Aragonite X-ray Fluorescence.
The XRF spectrum of aragonite, $CaCO_3$, measured with the CUBIC CCD, which shows the presence of the carbon and oxygen lines.

To find the weight proportions of the minerals that best match the measured XRD data, we must vary the ratios in which the calculated minerals are mixed to reproduce the observed crystal pattern. These weight proportions are listed in Table 3, calculated for both the CHEMIN XRD pattern as shown in Figure 9 and for XRD data from the same sample collected on a laboratory diffractometer. The errors listed are calculated statistical errors of approximately 2θ. Note that the relative error varies not only with mineral abundance but also with mineral type.

Clearly some mineral abundances can be more precisely measured than others. For example, the feldspars are complicated by ternary cation exchange (Ca, Na, K) and associated framework Al/Si ratio variations. In addition, in high-alumina basalts such as this sample, they also form as phenocryst and groundmass phases, with separate exsolution histories, which results in superposed complex mixtures of high- and low-temperature structural types. Although this makes the feldspar calculations more error prone and, in this sample, of greater abundance than should be present (compare the calculated normative value in Table 3), in fact, the complexity of the pattern indicates a wealth of information.

It should also be noted that, in some respects, the Rietveld data are more accurate than a normative calculation. The normative calculation is exceptionally sensitive to SiO_2 content, and the norm shown in the third column of Table 3 reports less olivine and more oxide minerals than the sample petrography allows. This discrepancy reflects the magnitude of the errors commonly associated with instrumental determinations of SiO_2 content in rock samples. In this instance, the Rietveld determinations of mineral abundance are likely closer to reality. The XRD-based analysis also identifies phlogopite, which is not recognized in the normative calculation, and it does not assume spurious occurrences of ilmenite and hematite.

Conclusions

Our prototype CHEMIN instrument, which has been in operation since July 1996, has confirmed the principle of CCD-based simultaneous XRD and XRF. Unfortunately, some of the components in this prototype do not allow CHEMIN's full capabilities to be realized as they would be with an optimized instrument. Nevertheless, using CHEMIN, we have been able to detect and quantify minerals at abundances as low as 1%, as well as to provide quantitative chemistry and mineralogy from complex mixtures (Table 3). We have tested this instrument with numerous pure minerals and mineral mixtures to examine its potential in mineralogic characterization of extraterrestrial bodies. We have applied Rietveld refinement methods to XRD data to determine unit-cell parameters and quantitative phase information from <1-mg-sized samples. Combining Rietveld quantitative mineralogical analyses and XRF data on a single sample has the potential to provide accurate mineralogical data for remote or extraterrestrial samples. For example, such diffraction data would remove the ambiguity regarding the mineralogy of the Martian surface that results from the availability of chemical information only. ▪

Table 3. Rietveld Analyses of Basalt Using XRD Data from CHEMIN and a Laboratory Diffractometer Compared with a Normative Calculation (all data in weight percent; statistical error of ~2σ in parentheses)

	CHEMIN	Laboratory Diffractometer	Normative Calculation
forsterite	7.5 (3.0)	9.3 (2.0)	2.7
albite	28.09 (7.0)	22.2 (5.0)	35.2
anorthite	17.5 (5.0)	27.3 (3.0)	20.7
sanidine	37.9 (8.0)	28.8 (6.0)	17.5
augite	4.7 (2.0)	9.3 (2.0)	10.5
magnetite	1.9 (1.0)	1.1 (1.0)	3.3
ilmenite	—	—	3.4
hematite	—	—	4.2
fluorapatite	1.6 (1.0)	2.1 (1.0)	2.3
phlogopite	0.1 (0.1)	0.1 (0.1)	—

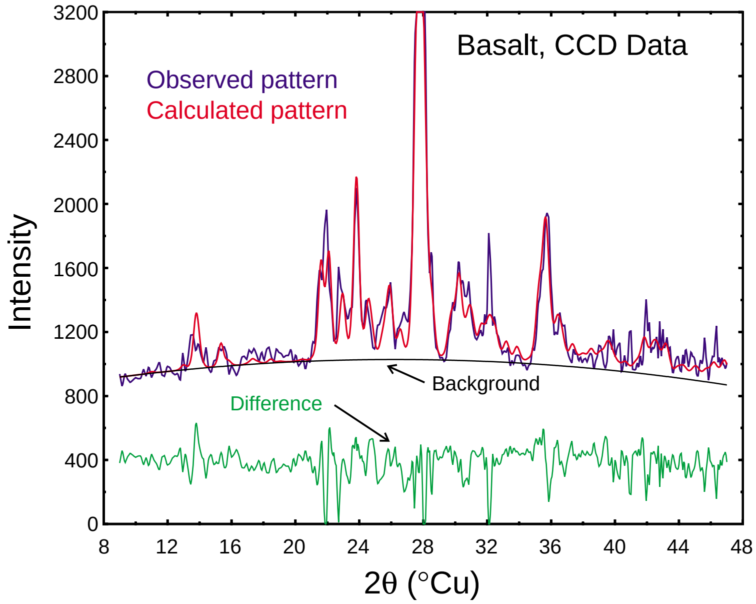

Figure 9. Rietveld Refinement of Basalt Diffraction Using CHEMIN. Observed diffraction data are blue, the pattern calculated based on the crystal structures of the component minerals is red, the difference between the calculated and observed patterns is green, and the calculated background is black.

Further Reading

Bish, D. L., and J. E. Post. 1989. *Modern Powder Diffraction. Reviews in Mineralogy*, vol. 20, 369 pp. Washington, D.C.: Mineralogical Society of America.

Bish, D. L., and J. E. Post. 1993. Quantitative mineralogical analysis using the Rietveld full-pattern fitting method. *American Mineralogist* **78**: 932–942.

Blake, D. F., et al. 1992a. Design of an x-ray diffraction/x-ray fluorescence instrument for planetary applications. *Lunar and Planetary Science Conference* **XXIII**: 117–118.

Blake, D. F., et al. 1992b. CHEMIN: Chemical and mineralogical analysis for planetary exploration using combined x-ray fluorescence and x-ray diffraction. *Discovery Mission Workshop, San Juan Capistrano, CA.*

Blake, D. F., et al. 1993. X-ray diffraction apparatus. U.S. Patent No. 5,491,738.

Blake, D. F., et al. 1994. A mineralogical instrument for planetary applications. *Lunar and Planetary Science Conference* **XXV**: 121–122.

Clark, B. C., and D. C. VanHart. 1981. The salts of Mars. *Icarus* **45**: 370–378.

Fegley, B., Jr., A. H. Treiman, and V. L. Sharpton. 1992. Venus surface mineralogy: Observational and theoretical constraints. *Proceedings of Lunar and Planetary Science* **22**: 3–19.

Kraft, R. P. 1994. Soft x-ray spectroscopy using charge-coupled devices with thin poly gates and floating gate output amplifiers. *Proceedings of SPIE—The International Society for Optical Engineering* **2280**.

Rietmeijer, F. J. M. 2000. What we can expect to learn from robotic exploration of a comet nucleus surface. In *Space 2000, Proceedings of the Conference, American Society of Civil Engineers, February 27-March 2, 2000, Albuquerque, New Mexico*, pp. 695–702.

Spindt, C. A. 1992. Microfabricated field-emission and field-ionization sources. *Surface Science* **266**: 145–154.

Vaniman, D. T., et al. 1991a. Integrated XRD and XRF data from a single instrument for planetary surface exploration. *Clay Minerals Society 28th Annual Meeting* 157.

Vaniman, D. T., et al. 1991b. In-situ planetary surface analyses: The potential of x-ray diffraction with simultaneous x-ray fluorescence. *Lunar and Planetary Science* **XXII**: 1429–1430.

Vaniman, D. T., D. Bish, D. Blake, S. A. Collins, P. Sarrazin, S. T. Elliott, and S. Chipera. 1998. Landed XRD/XRF analysis of prime targets in the search for past or present Martian life. *Journal of Geophysical Research, Planets* **103**: 31, 477–431, 490.